J Solid State Electrochem (2010) 14:1499–1508
DOI 10.1007/s10008-009-0973-4

ORIGINAL PAPER

Dissolved carbon dioxide effect on the behavior of carbon steel in a simulated solution at different temperatures and immersion times

Yamina Louafi · Mohamed Arezki Ladjouzi · Kamel Taibi

Received: 22 July 2009 / Revised: 27 October 2009 / Accepted: 28 October 2009 / Published online: 11 December 2009

Abstract Dissolved carbon dioxide effect on the behavior of carbon steel (0.4%carbon), in a simulated solution at different temperatures and immersion times, has been investigated using different techniques as potentiodynamic polarization, linear polarization resistance, and electrochemical impedance spectroscopy. The observation of the steel surface was done by scanning electron microscopy. All measurements reveal that the corrosion resistance is strongly dependent on both the temperature and immersion times. The corrosion resistance of carbon steel decreases in the solution considered as the temperature increases from 20 °C to 50 °C. Potentiodynamic polarization curves showed that cathodic and anodic current densities increase with the increased temperature. Besides, the study concluded that the addition of CO_2 gas to the simulated solution affects negatively the corrosion resistance in one hand and that, on the other hand, the higher the time of immersion the higher is the resistance to corrosion.

Y. Louafi (✉) · M. A. Ladjouzi
Laboratoire d'électrochimie, corrosion,
métallurgie et de chimie minérale, Faculté de Chimie,
Université des Sciences et Technologies Houari Boumédiène,
Bab-Ezzouar,
Algiers, Algeria
e-mail: elouafiamina@yahoo.fr

M. A. Ladjouzi
e-mail: M.Ladjouzi@yahoo.fr

K. Taibi
Faculté de Genie Mécanique,
Université des Sciences et Technologies Houari Boumédiène,
Bab-Ezzouar, Algiers, Algeria
e-mail: kameltaibi@yahoo.fr

Keywords Carbon steel · Corrosion · Simulated solution · Carbon dioxide · EIS

Introduction

Carbon steel is widely used as tubing or pipeline steel in the oil as well as in the gas industry, and it is usually strongly corroded, mainly when the electrolyte contains CO_2 [1].

The effects of environment, materials, and corrosion scale on the carbon dioxide corrosion have been reported in many papers [2–4].

CO_2 corrosion is a complex process, characterized by pit damages in petroleum extraction and transportation systems such as pipeline and related equipments.

Crolet reports [5] that carbon dioxide causes pitting in pipeline steel and increases both generalized and localized corrosion. It was also established that the added bicarbonate anions to the chloride solution increases the pitting potential of carbon steel.

Depending on whether the solubility of protective scale (such as iron carbonate or other salts) is exceeded or not, temperature can either increase or decrease the corrosion rate [6]. Xu et al. [7] suggested that when the temperature and HCO_3^- species concentration are lowered, the corrosion rate decreases due to inhibition of cathodic reactions.

On the other hand, Hurlen et al. [8] showed that the rate of cathodic reaction in the absence of CO_2 is affected not only by the buffer capacity but also by the pH of the solution. The study of Videm et al. [9] indicated that HCO_3^- ions could increase the pH which thus decreases the corrosion rate of carbon steel.

The temperature accelerates all the processes involved in CO_2 corrosion including transport of species, chemical reactions in the solution, and electrochemical reactions at the metal surface [10].

Several searchers [11, 12] suggested that the cathodic reaction controls the overall rate of corrosion in CO_2-saturated solution at temperatures below 60 °C, and the corrosion rate increases with the partial pressure of the CO_2 gas. According to Schmitt [13], the highest susceptibility to pitting corrosion occurred in the temperature range of 60–80 °C. When CO_2 dissolves into water, carbonic acid is formed under such conditions. This medium is more corrosive with respect to carbon steel than strong acid at the same pH in aqueous solution.

The aim of this paper is to evaluate the corrosion resistance of carbon steel in a highly chloride solution at different temperatures and immersion times, with and without the presence of CO_2 gas.

Experimental procedures

Materials

The working electrode was prepared from an N80 carbon steel cylinder the composition of which is listed in Table 1. The lateral surface of the cylinder was embedded in an epoxy resin, and only the base surface of 0.3 cm^2 was exposed to solution.

Surface preparation and solutions

The working electrode surface was polished first with silicon carbide abrasive paper up to 1,200, then rinsed with distilled water, degreased with acetone, and then the electrode was used immediately after. The corrosion behavior of carbon steel was evaluated in the temperature range of 20–50 °C.

The aggressive medium for testing the corrosion of carbon steel is a simulated solution prepared with various salts of analytical grade reagents and diluted in distilled water. Its composition is NaCl (48.53 g/l), $CaCl_2$ (5.10 g/l), and $NaHCO_3$ (0.503 g/l). It was deaerated for 30 min with pure N_2 and simultaneously saturated with CO_2 gas.

A saturated calomel electrode and a platinum electrode were used as reference and auxiliary electrodes, respectively. All measured potentials are referred to this reference electrode.

Measurements were performed using a Tacussel Radiometer PGZ 301 and controlled with Tacussel corrosion analysis software (Voltamaster 5).

Methods

Potentiodynamic polarization

The anodic and cathodic polarizations were realized separately from the free potential up to 400 mV/ECS at a rate of 1 mV/s. These experiments were conducted once maintaining the working electrode at its free potential during 30 min.

Electrochemical impedance spectroscopy

The EIS measurements were carried out after a 30 min constancy of the corrosion potential (E_{corr}) and at different times of immersion in simulated solution. Impedance spectra were obtained along the decreasing frequency range from 100 kHz to 10 mHz with ten points per decade. A sine wave with 10 mV amplitude was used to perturb the system. The charge transfer resistances (R_t) are calculated from the difference in impedance between lower and higher frequencies [14], and the double-layer capacitances (C_{dl}) are obtained using the frequency equation:

$$C_{dl} = \left(2f_c \prod R_t\right)^{-1}$$

where f is the frequency of the maximum imaginary component of the impedance $(-Z_{im})_{max}$.

Linear polarization resistance

The corrosion rate is directly related to linear polarization resistance (R_p) [15] which is a reliable parameter to the corrosion resistance. In addition, R_p is inversely proportional to corrosion current density i_{corr} leading to a correlation between the data obtained from the linear polarization resistance and those computed from Tafel plots. The linear polarization resistance (R_p) is deduced from the equation:

$$i_{corr} = B/R_p \quad (2)$$

It applies to E_{corr} with a scan rate of 1 mV/s and the Stern equation [16]. The resulting current is used to determine the corrosion current density

Table 1 Carbon steel composition

Elements	C	Mn	P	S	Si	Cu	Ni	Cr	Mo
Weight percentage	0.4	1.380	0.013	0.024	0.190	0.0940	0.03	0.09	0.190

Surface morphology

Corrosion morphology of surface steel was examined with scanning electron microscope (SEM JEOL JSM.6360 LV) using backscattered and secondary electrons as well as EDX analysis.

Results and discussion

Temperature effect

Potentiodynamic polarization curves

Figure 1a, b show the cathodic polarization curves for carbon steel immersed during 30 min in the studied electrolyte, respectively, in the absence and presence of carbon dioxide gas at different temperatures.

The shapes of the cathodic polarization curves are not affected by increasing temperature. This means that the nature of electrode processes is not modified. Cathodic current densities increase slightly with increasing temperature. This of course can be related to the acceleration of the electrode reaction. Many authors suggested that the cathodic reaction can be summarized by four steps (Eqs. 3a, 3b, 3c, 3d) [17, 18].

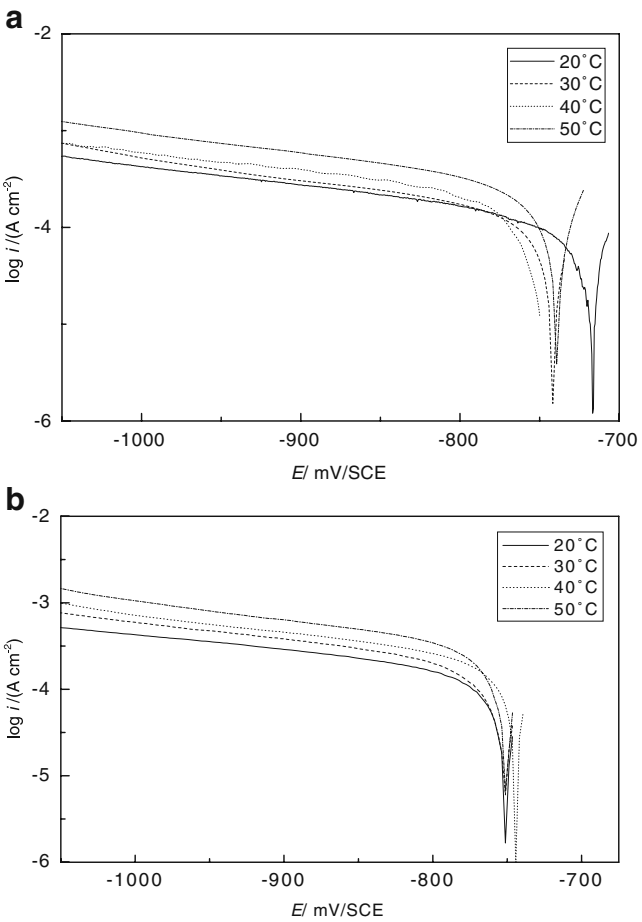

Fig. 1 **a** Cathodic polarization curves of carbon steel in the CO_2-free solution at different temperatures. **b** Cathodic polarization curves of carbon steel in the CO_2-saturated solution at different temperatures

$$2H^+ + 2e \rightarrow H_2 \quad (3a)$$

$$2H_2CO_3 + 2e \rightarrow H_2 + 2HCO_3^- \quad (3b)$$

$$2HCO_3^- + 2e \rightarrow H_2 + 2CO_3^{2-} \quad (3c)$$

$$2H_2O + 2e \rightarrow H_2 + 2OH^- \quad (3d)$$

In free-CO_2 solution, the direct reduction of HCO_3^- becomes the main cathodic process.

In the presence of carbon dioxide, the reduction of H^+ is the dominant cathodic process because the pH of the CO_2-saturated solution is low. At high overpotential, the dominant cathodic reaction converts towards a direct reduction of water (Eq. 4).

The anodic polarization curves of carbon steel in CO_2-free solution and in CO_2-saturated solution are reported in Fig. 2a, b, respectively. The general shape of the anodic polarization curves are not affected when increasing the temperature. However, the anodic polarization curves are displaced towards higher current densities as the temperature rises from 20°C to 50°C. Following the anodic polarization, a black layer was observed on the electrode in CO_2-saturated solution, which probably consists of $FeCO_3$, as reported by Ikeda [19]. This layer is more adherent when the temperature increases from 20°C to 50°C.

The anodic reaction is mainly due to the dissolution of iron (Eq. 4), which is followed by several steps

$$Fe \rightarrow Fe^{2+} + 2e \quad (4)$$

$$Fe^{2+} + CO_3^{2-} \rightarrow FeCO_3 \quad (5a)$$

$$Fe^{2+} + 2HCO_3^- \rightarrow Fe(HCO_3)_2 \quad (5b)$$

$$Fe(HCO_3)_2 \rightarrow FeCO_3 + CO_2 + H_2O \quad (5c)$$

During these processes a corrosion scale ($FeCO_3$) is formed on the surface of steel (Eq. 5a, 5c) as reported by Lopez [20]. The properties of these layers and their influence on the corrosion rate are important factors to be

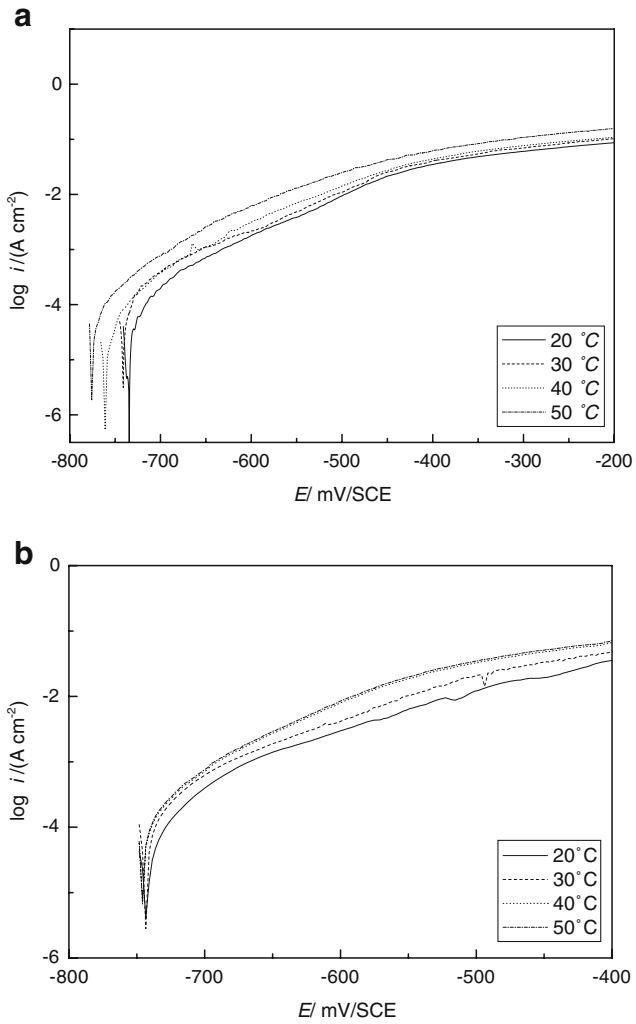

Fig. 2 **a** Anodic polarization curves of carbon steel in the CO_2-free solution at different temperatures. **b** Anodic polarization curves of carbon steel in the CO_2-saturated solution at different temperatures

taken into account when studying the corrosion of steel in CO_2-saturated solutions.

The electrochemical parameters (E_{corr}, i_{corr}, b_c, and b_a,) deduced from Tafel extrapolation plots are listed in Table 2, for CO_2-free solution and CO_2-saturated solutions.

In both cases, the corrosion potential (E_{corr}) is slightly affected from the increasing temperature, but more in the case of CO_2-free solutions, whereas the corrosion current density values i_{corr} increase when the temperature increases. The values of corrosion current densities of carbon steel in CO_2-free solution were smaller than those for the CO_2-saturated solution at each temperature. This indicates that the CO_2 gas is an accelerator of the steel dissolution (Table 2).

In the studied temperature range, no remarkable variation of anodic Tafel constant (b_a) is found. The values of cathodic slopes $|b_c|$ are high in both solutions, meaning that the cathodic reaction is strongly influenced by a diffusion process of species such as H^+, HCO_3^-, H_2CO_3, CO_3^{2-}

Analysis of surface morphology

Figure 3 shows the surface morphology of the corroded samples at different temperatures.

The analysis of these SEM images revealed that the corrosion product formed at the lowest temperature (20 °C) was not compact and easily peeled off from the carbon steel surface. By comparing Fig. 3a and b (same temperature but in CO_2-free and saturated free solutions, respectively), the corrosion product covers completely the surface of the corroded sample in CO_2-free solution. When CO_2 gas is added, the corrosion product is relatively regular and interstitial. The interspaces may be ways for diffusion of corrosion solution. The surface aspect of the surface at 50 °C is illustrated in Fig. 3c, d. Light areas represent the passivated surface and the dark ones the corrosion product, and the proportions show that almost all areas on this surface were seriously corroded as temperature increased.

Linear polarization resistance

The linear polarization curves $i=f(E)$ for steel without and with CO_2 gas are given, respectively, in Fig. 4a and b. The variation of current density versus potential is linear for both electrochemical systems. This linear variation is well described by the Stern equation [16], from which the polarization resistance values can be deduced.

Table 2 Electrochemical parameters deduced by Tafel methods for carbon steel in free-CO_2 solution and in CO_2-saturated solution at different temperatures

	T (°C)	E_{corr} (mV/SCE)	i_{corr} (μA cm^{-2})	b_c (mV dec^{-1})	b_a (mV dec^{-1})
Free solution	20	−717	101	−477	88
	30	−741	125	−479	85
	40	−740	194	−476	84
	50	−744	269	−480	95
Saturated solution	20	−725	144	−495	80
	30	−741	193	−505	99
	40	−745	239	−537	99
	50	−744	331	−490	104

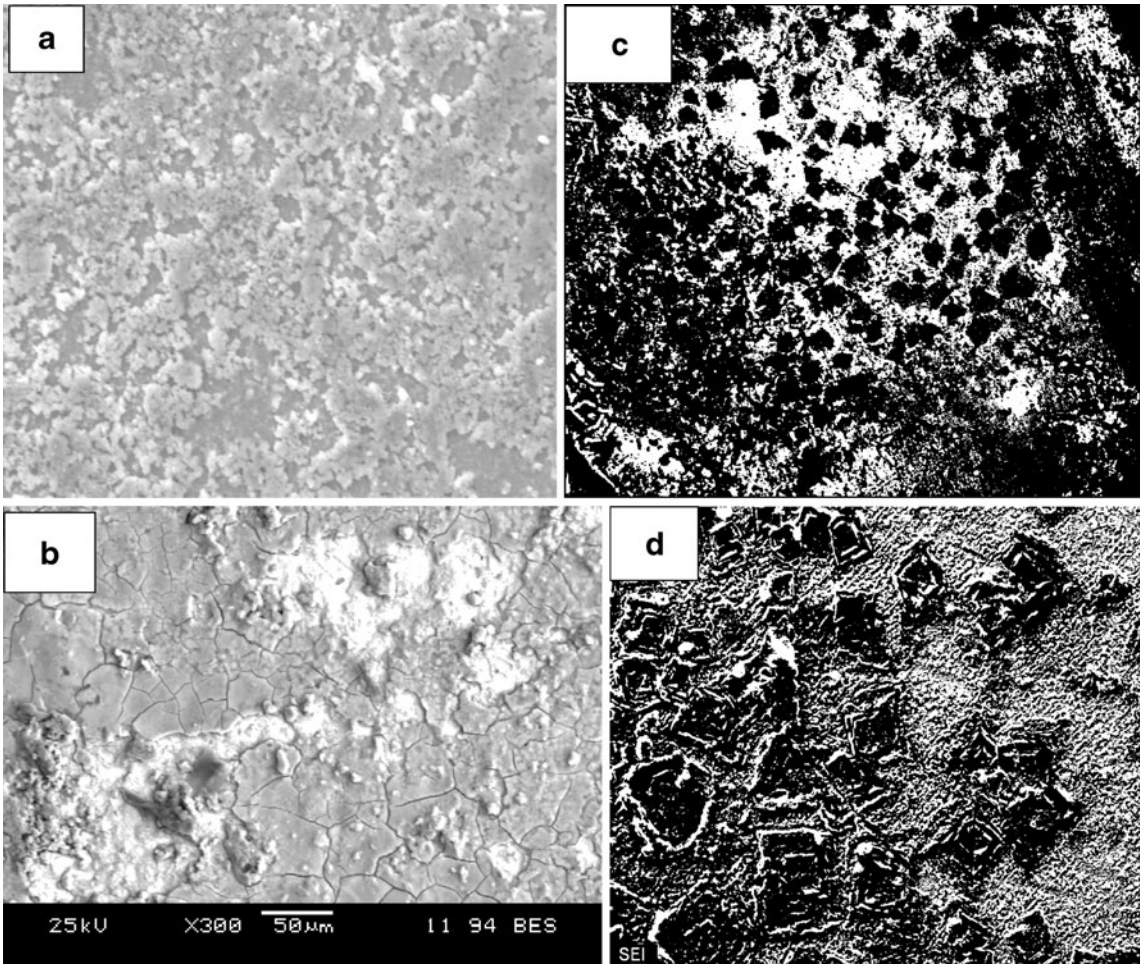

Fig. 3 SEM images of corroded surface of carbon steel immersed in the CO_2-free solution: 20 °C (**a**) 50 °C (**c**) and in the CO_2-saturated solution: 20 °C (**b**) 50 °C (**d**)

The electrochemical parameters obtained by the linear polarization technique are listed in Table 3. The second column gives the corrosion potential whereas the third one represents the polarization resistance, and the last one proposes the deduced corrosion rate from R_p.

It is clear from this results that with increasing temperature, i_{corr} increases and the polarization resistances (R_p) decrease.

The reported values of i_{corr} are in good agreement with those obtained from Tafel slopes.

Electrochemical Impedance Spectroscopy measurements

To confirm the potentiodynamic polarization results and to get a better understanding of the effect of CO_2 on corrosion behavior of carbon steel, EIS measurements were carried out in a simulated solution at different temperatures from 20 °C to 50 °C. Fig. 5a shows the Nyquist representations of impedance diagrams obtained in CO_2-free solution. The size of these impedance spectra are strongly influenced by different temperatures. Nyquist plots observed in Fig. 5a present one depressed semicircle at high frequency (HF) which could be considered as the capacitance of the double-layer between the corrosion scale and electrode [21]. The associated capacitance to this layer has value equal to 83 μFcm^{-2} at 50 °C of the usual double-layer capacitance [22]. The diameters of the Nyquist semicircles decrease with the increase of temperature. However, in the representation log Z_{im}=f(Log$f$), a straight line with slope nearly equal to 0.5 at all temperatures was seen (Fig. 5b). This observation reveals the existence of Warburg-type impedance.

On the other hand, secondary semicircles in the EIS Nyquist plots or a second-time constant in the EIS Bode plot Fig. 5b appeared at middle frequencies would be expected if a protective $FeCO_3$ corrosion product was forming on the surface.Warburg impedance appeared clearly at a very low frequency: it is a characteristic of the diffusion process.

Nyquist plots vs temperature in CO_2-saturated solution is shown in Fig. 6a. Warburg-type impedances are always observed in the high-frequency (HF) range. Values of n (Eq. 6) are found equal to 0.52, meaning that the

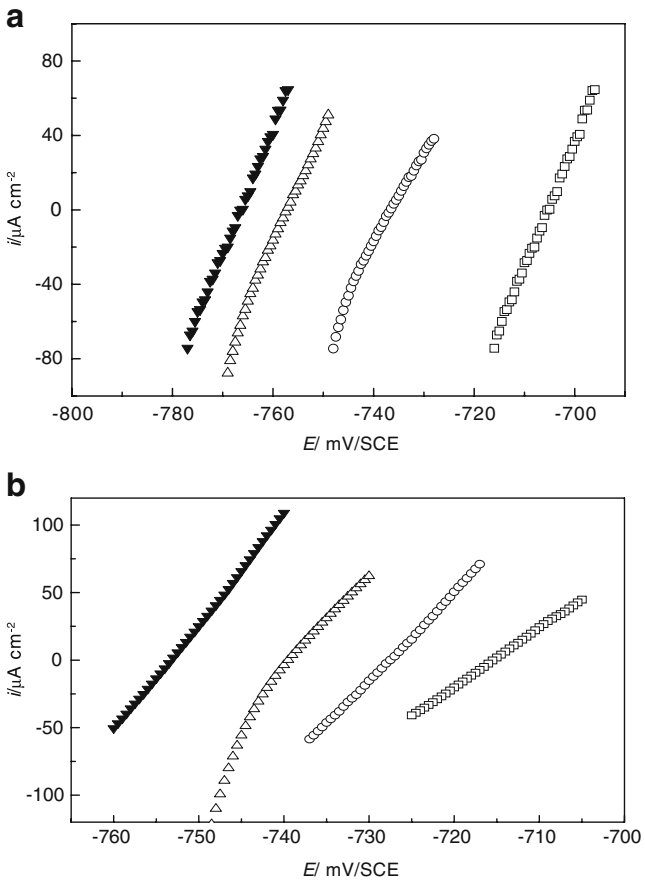

Fig. 4 **a**. Linear polarization curves of carbon steel in the CO_2-free saturated solution at different temperatures: *open squares* 20°C, *open circles* 30°C, *open triangles* 40°C, *closed inverted triangle* 50°C. **b** Linear polarization curves of carbon steel in the CO_2-saturated solution at different temperatures *open squares* 20°C, *open circles* 30°C, *open triangles* 40°C, *closed inverted triangle* 50°C

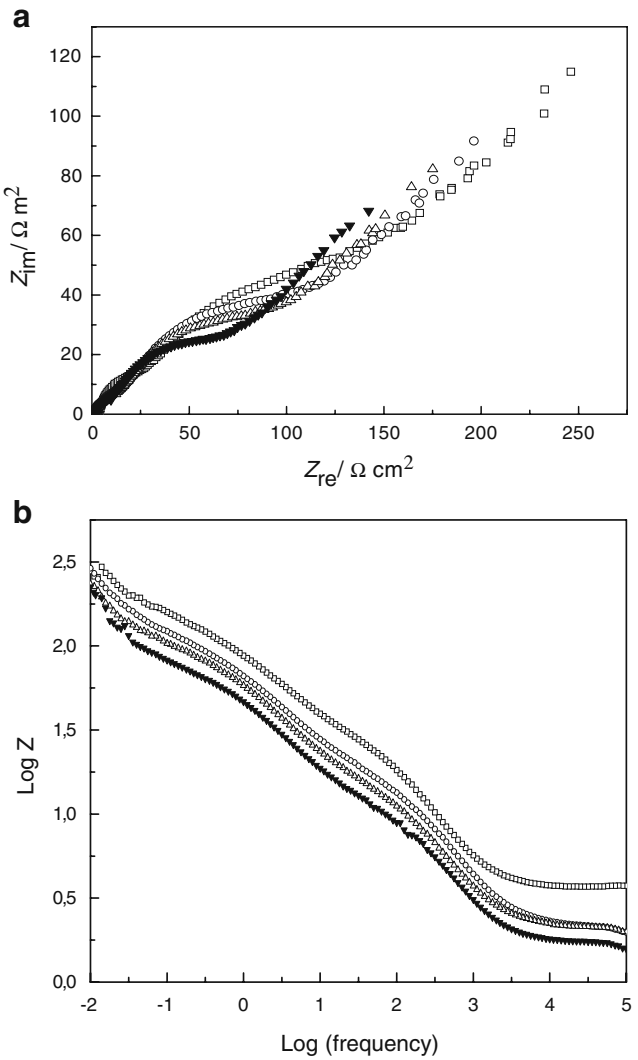

Fig. 5 **a** EIS of carbon steel in the CO_2-free solution at different temperatures *open squares* 20°C, *open circles* 30°C, *open triangles* 40°C, *closed inverted triangle* 50°C. **b** Bode diagram of carbon steel in the CO_2-free solution at different temperatures *open squares* 20°C, *open circles* 30°C, *open triangles* 40°C, *closed inverted triangle* 50°C

surface is heterogeneous. However, the diameters of the Nyquist semicircles decrease with the increase of temperature, inducing that the corrosion rate increases when temperature rises. A second capacitive semicircle or a second-time constant in the EIS Bode plot [Fig. 6b] is not quite observed. This may be due to the formation of a porous thin layer of $FeCO_3$. Nevertheless, Warburg impedance appeared clearly at a very low frequency; generally, it is a characteristic of diffusion process. The diagrams obtained in the CO_2-saturated solution are not significantly different from those obtained in the CO_2-free experiment.

Table 3 Electrochemical parameters deduced by LPR for carbon steel in free -CO_2 solution and in CO_2-saturated solution at different temperatures

	T (°C)	E_{corr} (mV/SCE)	R_p (Ω cm^2)	i_{corr} (μA cm^{-2})	B (mV dec^{-1})
Free solution	20	−706	252	128	32.4
	30	−738	200	156	31.3
	40	−757	170	184	31.4
	50	−766	150	230	34.5
Saturated solution	20	−717	224	133	30
	30	−738	152	236	36
	40	−742	145	248	36
	50	−752	134	276	37

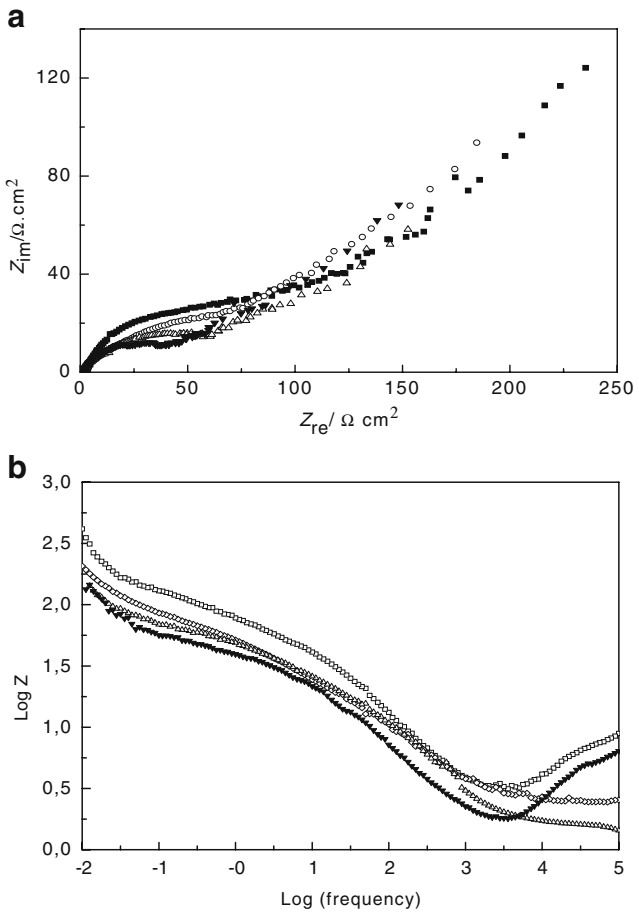

Fig. 6 **a** EIS of carbon steel in the CO_2-saturated solution at different temperatures *open squares* 20°C, *open circles* 30°C, *open triangles* 40°C, *closed inverted triangle* 50°C. **b** Bode diagram of carbon steel in the CO_2-saturated solution at different temperatures *open squares* 20°C ,*open circles* 30°C, *open triangles* 40°C, *closed inverted triangle* 50°C

All experimental plots have a severely depressed semicircular (HF) shape in the complex impedance plane, with the center lying below the real axis. This behavior is typical of solid metal electrodes that show a frequency dispersion of the impedance data [23]. Electrically equivalent circuits are generally proposed to simulate the electrochemical behavior. The most widely used is a constant phase element (CPE), which has a non-integer power dependence on the frequency. The impedance of a CPE is expressed by the relation:

$$Z_{\mathrm{CPE}} = Y^{-1}/(j\omega)^{-n} \tag{6}$$

where Y is a proportional factor, j is an imaginary number, ω is equal to $2\Pi f$, and n has the meaning of a phase shift [23]. CPE is often used in place of a capacitor to compensate deviations from ideal dielectric behavior associated with the non-homogeneous electrode surface.

However, Y values were determined from the constant phase element values Q_{dl} (Table 4) using Boukamp's expression [24]:

$$C_{\mathrm{HF}} = (YR_{\mathrm{HF}})^{1/n}/R_{\mathrm{HF}} \tag{7}$$

where C_{HF} and R_{HF} are the capacitance and the resistance at high frequency, respectively. The equivalent circuit of Fig. 7 has been proposed in the literature to study the carbon steel corrosion process in CO_2 medium [10]. This circuit describes the corrosion process in two simultaneously occurring stages. Here, R_s is the solution resistance, Q_{dl} is a constant phase element of the double-layer capacitance, R_t is the charge transfer resistance and capacitance, (R_2) and Z_w are the Warburg diffusion impedances.

Various impedance parameters such as corrosion potential, charge transfer resistance (R_t), double-layer capacitance (C_{dl}), and proportional factor Y are given in Table 4. The charge transfer resistance and double-layer capacitance values were calculated as described in Methods.

It can be noticed that the double-layer capacitance (C_{dl}) and Y increase with decreasing charge transfer resistance (R_t). This is related to the occurrence of a corrosion scale due to the dissolution of steel which increases its active surface. According to Turgoose et al. [25], this increase in the capacitance (Y) value is associated with an increase in the surface area available for the cathodic reaction, which is related to the electrochemical activity of the non-oxidized cementite (Fe_3C) residue exposed after the corrosion process. However, this would lead to a decrease in the

Table 4 Electrochemical parameters deduced by EIS methods for carbon steel in free-CO_2 solution and in CO_2-saturated solution at different temperatures

	T(°C)	E_{corr} (mV/SCE)	R_t (Ωcm^2)	C_{dl} (μFcm^{-2})	Y (μFcm^{-2})	Number (n)
Free solution	20	−732	33	63	15.8	0.47
	30	−753	24	64	21.5	0.48
	40	−768	20	78	26.5	0.52
	50	−767	15	85	33.2	0.5
Saturated solution	20	692	58	76	20.9	0.55
	30	−725	26	78	37.6	0.52
	40	−756	24	178	40.3	0.52
	50	−763	15	182	55.8	0.56

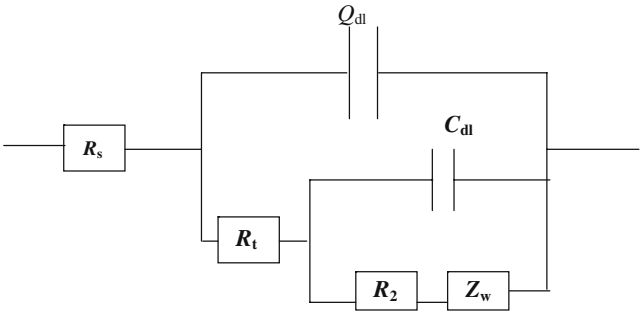

Fig. 7 Equivalent circuit model for the metal covered by porous corrosion product

values of R_t with increase of the temperature (higher corrosion rates). It is clear that the increase of temperature from 20°C to 50°C maintains the n factor values almost constant.

Potentiodynamic polarization technique or EIS were used to evaluate the corrosion resistance of carbon steel in a simulated solution saturated with carbon dioxide. The results are:

(1) The free corrosion potential of steel in both CO_2-saturated solution and CO_2-free solution shifts to more positive values when the temperature increases from 20°C to 50°C; (2) The values of corrosion current density (i_{corr}) of carbon steel in the CO_2-free solution were smaller than those for the CO_2-saturated solution; (3) corrosion resistance of steel in both CO_2 solution and free solution decreases when temperature increases from 20°C to 50°C; (4) the increase of temperature does not modify the corrosion process. (5) The corrosion process was not affected by the presence of CO_2 gas.

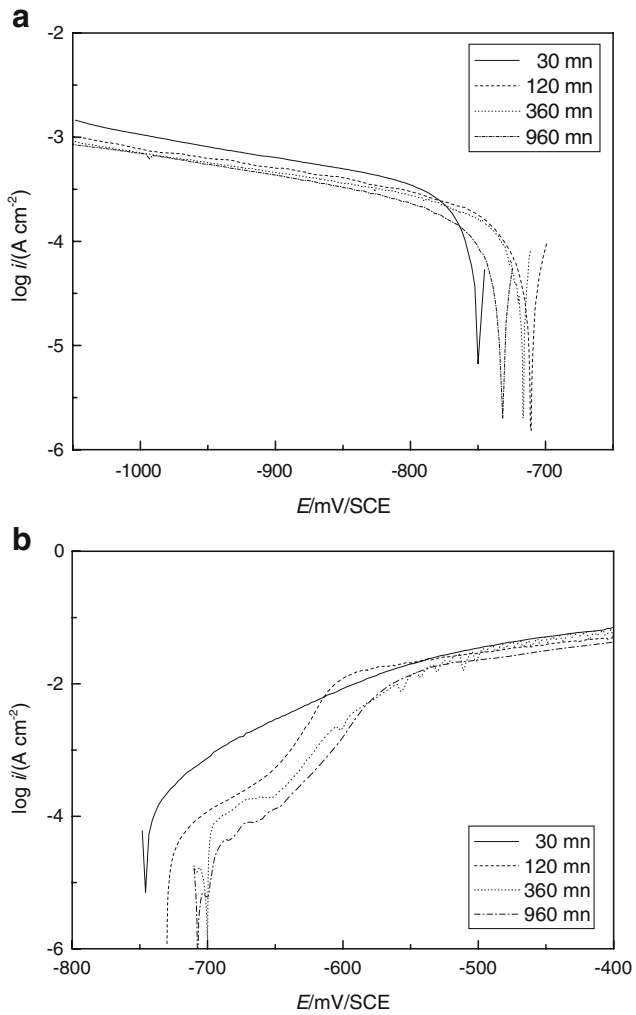

Fig. 8 **a** Cathodic polarization curves of carbon steel in the CO_2-saturated solution at different of immersion times. **b** Anodic polarization curves of carbon steel in the CO_2-saturated solution at different immersion times

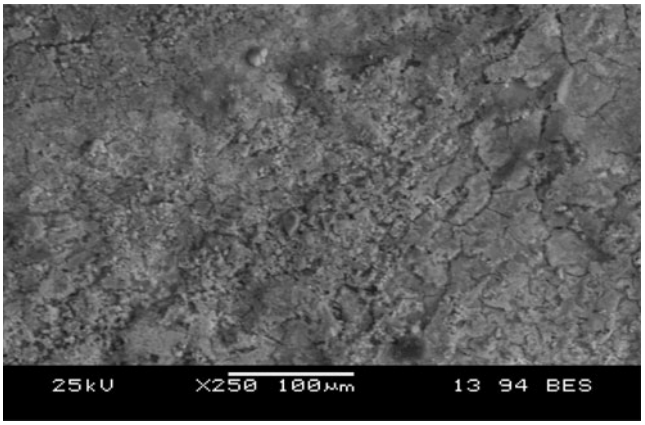

Fig. 9 SEM image of corroded surface of carbon steel immersed in the CO_2-saturated solution at 50°C during 960 min

Effect of the immersion time at 50°C

The immersion time effect of steel in the simulated solution saturated with carbon dioxide systems at 50°C is determined using potentiodynamic polarization (Fig. 8a, b), and electrochemical impedance spectroscopy are given in Fig. 9.

Potentiodynamic polarization curves

According to Fig. 8a, the shape of polarization cathodic curves of carbon steel in the considered solution is not

Table 5 Electrochemical parameters deduced by Tafel methods for carbon steel in CO_2-saturated solution at 50°C after different immersion times

Time (min)	E_{corr} (mV/SCE)	i_{corr} (μA cm^{-2})	b_c (mV dec^{-1})	b_a (mV dec^{-1})
30	−752	331	−490	104
120	−720	213	−416	65
360	−715	205	−459	97
960	−726	182	−418	73

affected by the increased immersion time. It can be seen that the cathodic curves are displaced towards lower current densities with the increase of immersion time from 30 min to 960 min. The anodic current density decreases gradually in the active zone with increasing immersion times which are related to compaction and integration of corrosion scales [3] (Fig. 8b).

Table 5 gives the electrochemical parameters E_{corr}, i_{corr}, b_c, and b_a. The small shift of E_{corr} with immersion time can be explained in terms of the formation of a thick layer [26]. The main result is that corrosion current density values decrease slightly between 30 and 960 min, revealing thus that the continuous immersion makes the surface of the carbon steel more protective.

The aspect of the metallic surface after 960 min is illustrated in Fig. 9, and it shows that almost all the area of the scanned surface was entirely covered with the corrosion product, and the latter is rougher, compact and presents porous characteristics. This is coherent that the corrosion resistance is increasing with the exposure time.

Electrochemical impedance spectroscopy

Figure 10 shows the effect of immersion time in the Nyquist plots in a carbon dioxide-saturated solution at 50 °C. Nyquist plots measured at each exposure time presents with tails at low-frequency range. The tails are inclined with an angle of 50° with respect to the real axis at very low frequencies. This means that for each exposure time, the diffusion process of ions occurs on the electrode. According to previous work [27], the diffusion is due to the produced formation porous layer on the surface. From

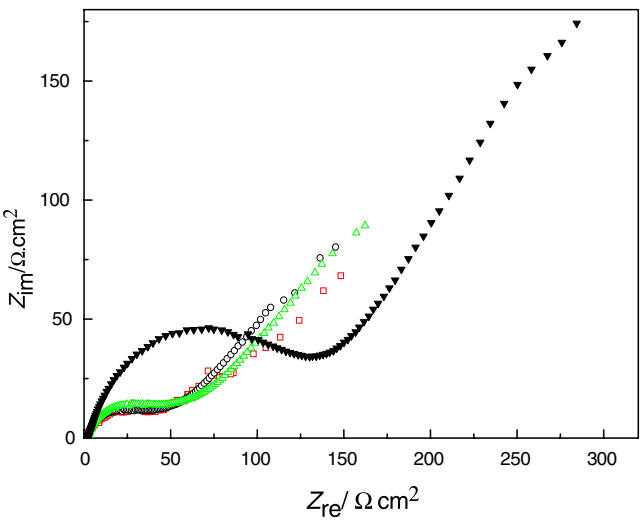

Fig. 10 EIS of carbon steel immersed after different times in the CO_2-saturated solution *open squares* 30 min; *open circles* 120 min; *open triangles* 360 min; *closed inverted triangle* 960 min

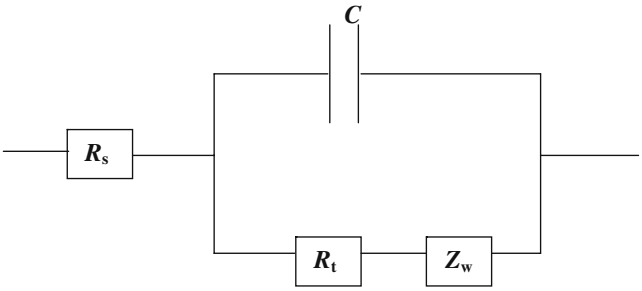

Fig. 11 Simplified equivalent circuit model for the metal covered by porous corrosion product $C=C_f+C_{dl}$ (C_f is the film capacitance)

Fig. 10, it can be also observed that the diameter of depressed semicircle increases with increasing times. This means that the corrosion rate becomes lower at a long exposure time.

These results are in good agreement with Cui et al. [3] who suggested that the corrosion scale became compact and adhesive with the increase of the exposure time as well as temperature. It can be concluded that, at the first stage of corrosion, addition of CO_2 raises the corrosion rate, but the latter decrease after the occurring of corrosion scale while the electrode reaction process is controlled by ion diffusion in the corrosion scale. When the steel corrosion process is accompanied by the formation of porous layer of corrosion product, Chen and Hong [10] ascribe the equivalent circuit elements in Fig. 11 to these two stages.

The impedance parameters deduced from the diagrams of Fig. 8 are summarized in Table 6. The results obtained prove that the values of R_t and C_{dl} increase with the increasing immersion times of carbon steel in CO_2-saturated solution. Consequently, an increase in the capacitance value could be related to the growing area due to iron carbonate deposit over the whole surface of carbon steel, and this comes with an increase in the corresponding R_t values.

Finally, it can be seen that there is a good agreement between the potentiodynamic polarizations and impedance techniques leading the same effects of temperature and immersion time.

Table 6 Electrochemical parameters deduced by EIS methods for carbon steel in CO_2-saturated solution at 50°C after different immersion times

Time (min)	E_{corr} (mV/SCE)	R_t (Ω cm^2)	C_{dl} (μF cm^{-2})
30	−767	15	182
120	−716	68	233
360	−716	76	323
960	−712	115	355

Conclusions

In this study, the effect of dissolved carbon dioxide on the behavior of carbon steel in simulated solution at different temperatures and immersion times was investigated using electrochemical potentiodynamic polarization, linear polarization resistance, and electrochemical impedance spectroscopy.

The behavior of steel in simulated solution depends on the temperature and immersion times.

The carbon steel has a better corrosion resistance in CO_2-free simulated solution than in the CO_2-saturated solution. Increasing the temperature affects negatively the corrosion resistance of carbon steel in CO_2-saturated solution and in CO_2-free solution.

This study allows us to conclude that the higher the immersion time the higher is the resistance to corrosion. At the first stage of corrosion, addition of CO_2 accelerates the corrosion rate, whereas the latter decreases after occurring of the corrosion scale.

References

1. Johnson M, Tomson M (1991) Proceedings of NACE Corrosion 268
2. Ren C, Liu D, Bai Z, Li T (2005) Mater Chem Phys 93:305
3. Cui ZD, Zhu SL, Yang XJ (2006) Appl Surf Sci 252:2368
4. Parkins RN, O'Dell CS, Fessler RP (1984) Corros Sci 24:343
5. Crolet JL (1994) Predicting CO_2 corrosion in the oil and gas industry
6. Nesic S, Nordsween M, Nyborg R, Stangeland A (2001) Corrosion, NACE 40
7. Xu LM, Dong ZH, Fan HX (1996) Effect of CO_2, HCO_3^- on the corrosion of carbon steel in oil and gas fields productive water. Nat Gas Ind 4:57
8. Hurlen T, Gunvaldsen S, Tunold R, Blaker F, Lunde PG (1984) J Electroanal Chem 18:511
9. Videm K, Koren AM (1993) Corrosion, passivity, and pitting of carbon steel in aqueous solutions of HCO_3^- CO_2 and Cl^-. Corrosion 49:746
10. Yen ZF, Zhao WZ, Ba Q, Fing ZYR (2008) Electrochemica Acta 53:3690
11. Ikeda A, Ueda M, Mukai S, Hausler R, Giddard HP (1984) Advances in CO_2 corrosion. Nace 1:39
12. Schmitt G, Hausler RH, Giddard HP (1984) (Eds) Advances in CO_2 corrosion, NACE 1
13. Schmitt G (1985) Advances in CO_2 corrosion, NACE 1
14. Tsuru T, Huruyama S, Gjutsu B, Japan J (1978) Soc Corros Eng 27:573
15. Uhling HH, Revie RW (1985) Corrosion and corrosion control. Wiley, New York, p 405
16. Stern M, Geary AL (1957) J Electrochem Soc 56:104
17. Ogundele GI, White WE (1986) Corrosion 42:71
18. Nesic S, Postlethwaite J, Olsen S (1996) Corrosion 52:280
19. Ikeda A, Ueda M (1994) in Predicting CO_2 corrosion in the oil and gas industry: 48
20. Lopez DA, Schreiner WH, de Sanchez SR, Simison SN (2003) Appl Surf Sci 20:769
21. Li DG (2007) Appl Surf Sci 253:8371
22. Truc TA, Pebere N, Hang TTX, Hervaud Y, Boutevin B (2002) Corros Sci 44:2055
23. Bilkova K, Hackerman N, Bartos M (2002) Proceedings of NACE 2284
24. Bouckamp BA (1993) Users manual equivalent circuit ver. 4.51, Faculty of chem. Tech. Universidad of Twente, The Netherlands
25. Mora-Mendoza JL, Turgoose S (2002) Corros Sci 44:1223
26. Zhang G, Lui M, Chai C, Wui Y (2006) Materials 13:44
27. Chen Y, Hong T, Gopal M, Jepson WP (2000) Corros Sci 42:979